ELSEVIER

Journal of Power Sources 67 (1997) 283–289

JOURNAL OF POWER SOURCES

Continuous casting of lead–antimony alloys

E. Cattaneo *, H. Stumpf, H.G. Tillmann, G. Sassmannshausen

Accumulatorenwerke Hoppecke, 59914 Brilon, Germany

Received 12 November 1996; accepted 31 December 1996

Abstract

Lead–calcium–tin (Pb–Ca–Sn) grids for lead/acid positive plates produced with alternative methods to mould casting have gained increasing acceptance during the last twenty years. Similar development of alternative lead–antimony (Pb–Sb) grids has been hampered by the poor electrochemical behaviour of these alloys as characterized by increased grid growth and abnormally high rates of open-circuit corrosion. Continuously-cast antimonial grids with corrosion and mechanical properties that match those of conventional, mould-cast types have been recently developed at Hoppecke. This paper gives an account of the associated development programme in the field. Different aspects of continuous casting of low-antimony alloys are discussed. © 1997 Elsevier Science S.A.

Keywords: Alloys; Lead; Tin; Calcium; Battery grids; Lead–antimony alloy corrosion; Continuously cast; Grid growth

1. Introduction

The production of plates for automotive batteries in a continuous process provides high productivity with low spread in weight and reduced amount of scrap [1]. A comparison of the development of the different continuous grid-manufacturing processes since the 1980s, shows that only antimony-free alloys, mainly lead–calcium–tin (Pb–Ca–Sn), have reached commercial application. By contrast, little progress has been made for the equivalent low lead–antimony alloys (Pb–Sb). Apart from a few successful attempts, the difficulties encountered have hampered the commercial introduction of continuously-cast antimonial positive grids. In this paper, an account is given of work by the author's company with the Wirtz continuous casting system ('Concast').

2. Early experience with the casting system

The Wirtz process [2] consists of feeding the molten lead through the orifices of a casting shoe onto a rotating drum. The melt freezes in the multiple grid engravings on the casting drum to form a continuous grid-band. The grid output is up to six times higher than that for conventional mould-casting procedures. A project was started at Hoppecke in 1992 with the goal of replacing the standard gravity-cast Pb–1.8Sb grids with concast Pb–1.8Sb grids in a similar way in which, a year before, concast Pb–Ca grids had replaced conventional ones. As shown below, this goal could not be achieved in a single step. Fig. 1 shows the main development stages — from the initial trials until the present status in which series-production of hybrid concast batteries has started.

The early Pb–1.8Sb grids produced with the concast process displayed poor metallurgical quality. Extensive hot-cracking (particularly at the wire intersections) and deep penetrating cold-welding on the drum side (Fig. 2) were typical deficiencies. On the shoe side, insufficient feeding of the melt in the grooves caused extended surface porosity (Fig. 3). To minimize these problems, changes in the casting shoe and other parts of the equipment were introduced. Since then, the macroscopic grid quality has been continuously improved.

3. Microstructure of early positive grids

The first batteries manufactured with positive concast antimonial grids of minimal metallurgical quality suffered abnormally high rates of open-circuit (OC) corrosion. This corroborated with the previous experience of other battery manufacturers. The early batteries also showed a higher self-discharge rate than the equivalent mould-casting types

* Corresponding author. Tel: +49-2963-61544; Fax: +49-2963-61260.

PII S0378-7753(97)02558-5

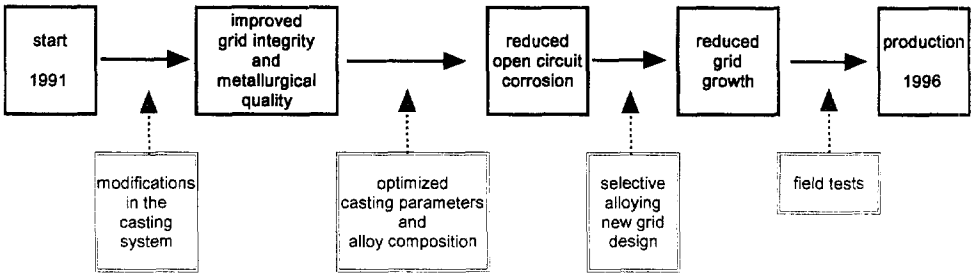

Fig. 1. Development steps in Hoppecke lead–antimony grid project.

with a simultaneous abnormal increase in the internal resistance (Fig. 4). The combination of grid growth and stress from the volume expansion of the active mass on these brittle grids caused plates literally to break into pieces after a few months storage.

One of the main concerns was the extreme low ductility and the tendency to hot-cracking — a known disadvantage of early mould-casting grids with antimony concentrations below 2.8 wt.% [3,4].

In the wide freezing range of these alloys, the build-up of the dendritic, lead-rich, primary-solid solution occurs in the presence of a second antimony-rich liquid phase. With decreasing antimony content, the dendritic grain size increases and the scarce surrounding liquid phase cannot compensate for the solidification shrinkage [5]. The result is extensive cracking. For continuously drum-cast antimony alloys (as mentioned in Ref. [6]), the situation is even worse.

Microstructural analysis of early concast grids (status 1992) showed a coarse, drum-shoe oriented grain structure (Fig. 5(a)). The columnar grains on the drum side (the colder side where nucleation starts) display a cellular substructure without dendrite side branching. By contrast, the smaller grains on the shoe side have coarse dendrites compared with the fine dendrites in the middle. These variations in dendrite size with corresponding irregular distribution of the antimony-rich inter-dendritic spacings, suggest different (local) solidification times along the heat flow direction [7].

It is worth mentioning that the variable grain sizes observed along the drum-shoe were not exclusive to concast Pb–Sb alloys. Fig. 6 shows the grain structure of a concast Pb–0.06Sr–0.25Sn alloy. As in the case of the concast Pb–0.8Sb microstructure shown in Ref. [8], a clear distinction can be made between a columnar-grained drum region and a fine-grained shoe region. The apparent simi-

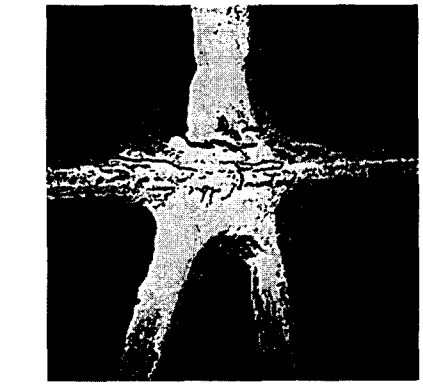

Fig. 2. Grid node of a corroded battery; concast Pb–1.8Sb grid (drum side) showing hot-cracking and cold-welding.

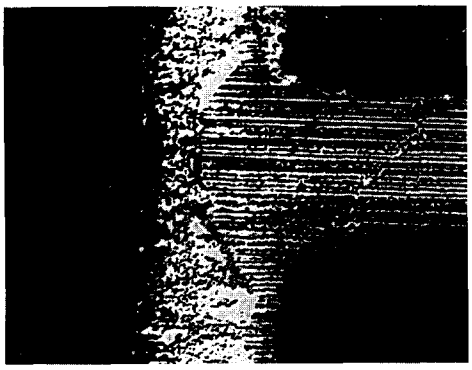

Fig. 3. Grid node of a concast Pb–1.8Sb grid (shoe side) showing extended surface porosity due to insufficient molten lead filling of the casting-drum grooves.

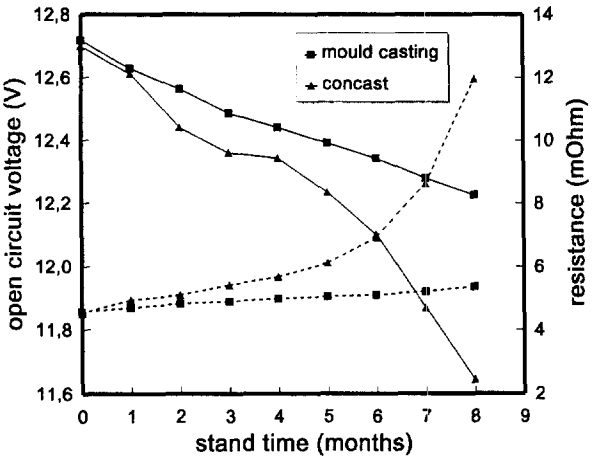

Fig. 4. Open-circuit storage test at room temperature. Time dependence of the voltage and the internal resistance for batteries made with continuously-cast and mould-cast Pb–1.8Sb positive grids.

Fig. 5. (a) Coarse-grain structure (× 100) of the upper frame cross section of a concast Pb–1.8Sb grid (status 1992) showing microstructural gradients in the drum-shoe direction. The sub-structure of the columnar grains in the drum region (bottom) is cellular. The smaller irregular grains of the shoe region (top) exhibit a dendritic substructure. (b) Coarse-grain structure (× 100) of the upper frame of a grid belonging to the same band. In this case, the small grain-size, shoe region shows a coarse globulitic substructure. The different behaviour to that in (a) suggests non-uniform cooling rates.

larity between structures cannot be extrapolated to the mechanical properties: the high ductility of the strontium alloy contrasts with the brittle low-antimonial version.

4. Microstructure with optimized casting conditions

Strong microstructural gradients were characteristic for the early concast grids which exhibited poor metallurgical and electrochemical properties. To match the corrosion stability and the mechanical properties of the gravity-cast grids, it was necessary to find suitable casting conditions, i.e., develop a way to obtain reproducible, homogeneous, fine-grained structures. This was achieved by means of: (i) a high cooling rate of the casting drum; (ii) effective amounts of nucleants in the alloy composition; (iii) suitable concast (specific) casting parameters.

The granular structure of the improved concast Pb–1.8Sb grid is shown in Fig. 7(a). A fine, regular structure with minimal gradients in grain size is obtained. Fig. 7(b) and 7(c) show the equivalent structures for a mould-cast Pb–1.8Sb alloy and an expanded Pb–1.53Sb alloy (status February 1992), respectively. The fine dendritic substructure of the concast Pb–1.8Sb is shown in Fig. 8(a), and the equivalent coarse dendrites of the mould-cast alloy in Fig.

Fig. 6. Grain structure (× 100) of a concast Pb–0.06Sr–0.25Sn alloy. The cross section exhibits columnar grains on the drum side (bottom) and finer more regular grains on the shoe side (top).

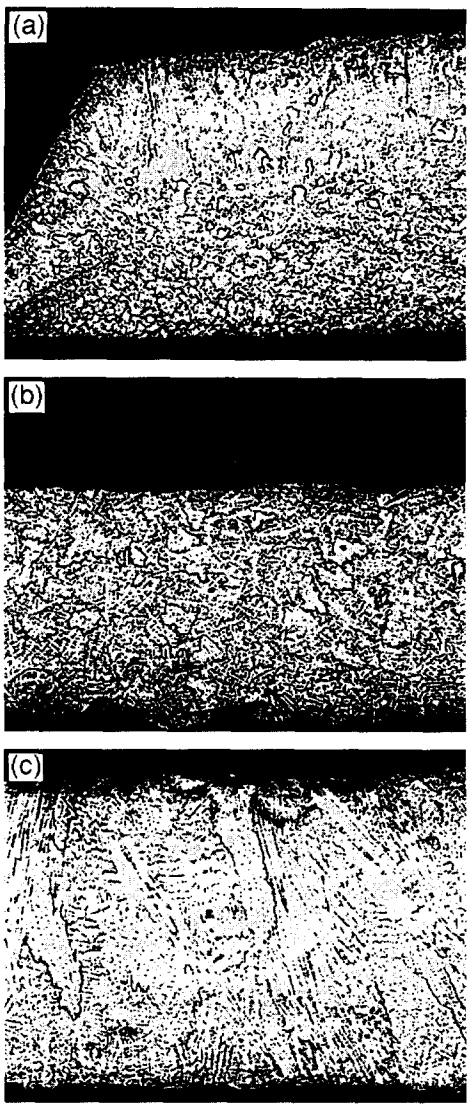

Fig. 7. Micrographs of three different antimonial alloys: (a) cross section (×50) of the 1.2 mm thick upper frame of improved concast Pb–1.8Sb alloy (status 1996) that exhibits a fine-grained structure with minimal gradients of grain-size (top: drum-side; bottom: shoe side); (b) coarse dendritic structure (×50) of a mould-cast Pb–1.8Sb grid grating; (c) cross section (× 100) of upper frame of a Pb–1.53Sb expanded grid that shows oriented grains in the drum-side/air-side.

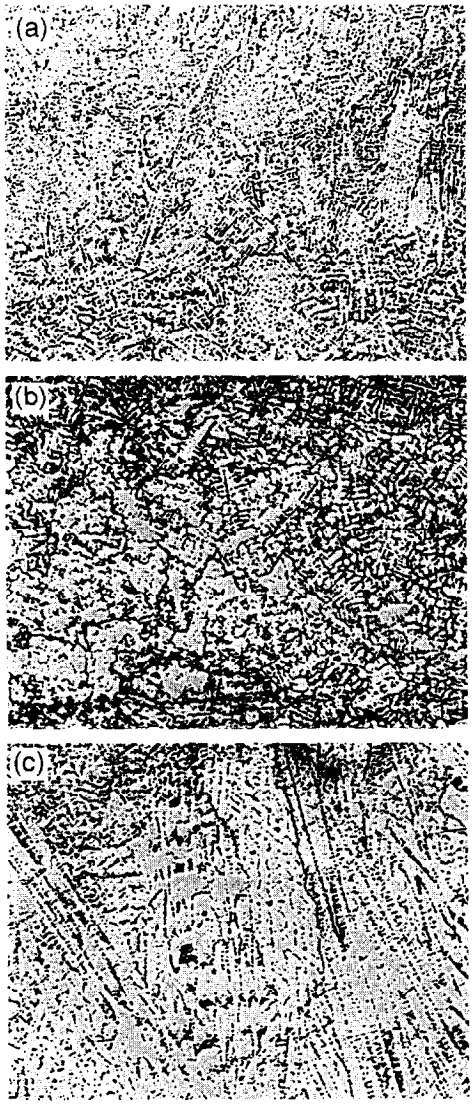

Fig. 8. Grain sub-structure of antimonial alloys of Fig. 7: (a) concast Pb–1.8Sb (×200): fine dendritic; (b) mould cast Pb–1.8Sb (×100): coarse dendritic; (c) expanded Pb–1.53Sb (×200): cellular (very little or no dendrite side branching).

8(b). The structures of the improved concast Pb–1.8Sb and the mould-cast Pb–1.8Sb alloys are qualitatively the same. The difference is the smaller scale in size.

The expanded Pb–1.53Sb, on the other hand, has a different granular structure which is characterized by elongated grains in the drum-air direction (Fig. 7(c)) with a cellular (or 'fibrous dendritic', as denoted in Ref. [7]) drum-air oriented sub-structure Fig. 8(c).

There is also an important difference in the alloy composition — the continuously cast Pb–1.53Sb strip (kindly supplied by the manufacturer) contains no nucleants. Until recently, all alloys were prepared with set, effective amounts of nucleants to control the grain size (different nucleants are discussed in Refs. [4,9,10]). The alternative of doing without nucleants relies on the grain-refinement effect from the enhanced cooling rate of the casting drum.

5. Open-circuit corrosion tests

Systematic, open-circuit (OC) corrosion tests were carried out to evaluate different casting conditions and alloy compositions. Batteries were discharged to 50% of their 20 h capacity (50% depth-of-discharge (DOD)) and stored at room temperature. The OC voltage, acid density and a.c. impedance (80 Hz) were monitored periodically. A 50% DOD corresponds to a H_2SO_4 density of 1.180 to 1.185 g cm^{-3}, i.e., the test starts at positive grid potentials of about 1.02 V versus Hg^+/Hg_2SO_4. This potential range is characterized by a high OC corrosion rate [11]. From this point, the acid density decreases steadily with the storage time, due to self-discharge, and the thickness of the $PbSO_4/PbO$ corrosion layer increases.

The data given in Fig. 9 show an almost linear time dependence of the weight losses for concast Pb–1.8Sb battery grids and mould-cast Pb–1.8Sb grids of the same battery type (the corrosion layer was removed in a mannitol/hydrazine solution). The fine-grained, continuously-cast grids and the conventional grids exhibit similar OC corrosion rates.

6. Grid growth

One of the advantages of the continuously-cast process is the possibility of manufacturing low-weight grids. Requirements placed upon the reduction of grid thickness are as follows:

- sufficient mechanical strength to allow plate processing
- predictible corrosion rates in terms of weight loss
- the absence of deep, penetrating (local) corrosion
- reduced grid growth

Grid growth is an important issue. It repeatedly arises when comparisons are made between alternative grid-processing methods and the traditional mould-casting for

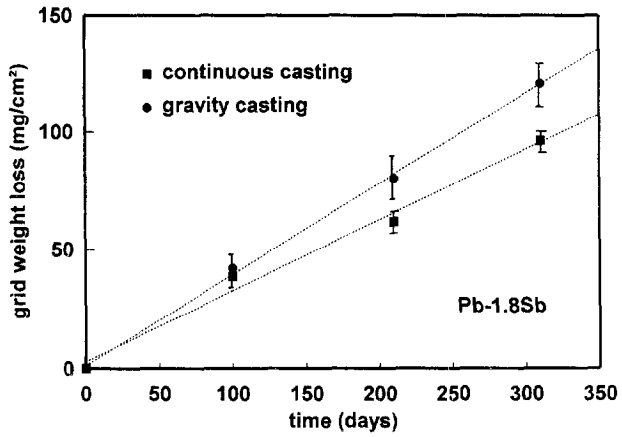

Fig. 9. Open-circuit storage battery test at room temperature [8]. Weight loss as a function of temperature for improved (fine grained) concast and conventional Pb–1.8Sb grids, respectively.

Fig. 10. Pb–1.8Sb concast battery grid with early design after a cycle-life test of 18 weeks and showing the typical grid growth deformation [8].

antimonial grids. Expanded antimonial lead alloys are no exception [6,12,13].

This phenomenon is a consequence of the (wedge-shaped) intergranular corrosion attack on the grid surface that results in a deforming tension along the grid gratings. The main failure mode of automotive batteries is ascribed to short-circuits [14].

Early concast Pb–Sb alloys produced in the authors' company showed higher rates of grid growth than conventional alloys. To reduce the dangers of directional vertical grid growth (a typical example is shown in Fig. 10), a new grid design was implemented (Fig. 11). In addition, through selective alloying (copper, tin), the disparity with mould-cast grids was reduced.

The evaluation of the effect of small variations in alloy composition exclusively through battery tests proved to be time-consuming. Therefore, to speed up the studies and to cover a wider range of alloy composition, comparatively rapid tests were performed on both pasted and bare grids. One of these tests consists in cycling bare grids for 60 days at 60 °C with the current profile shown in Fig. 12(a). The grids undergo different potentials as shown in Fig. 12(b) (the cut-off for discharge was set at 0.6 V versus Hg^{+}/Hg_2SO_4). Quantitative results were obtained by averaging single values of three identical cells connected in series. This experiment was carried out for a set of grids made from the alloys listed in Table 1. All these were continuously cast in the new grid design of Fig. 11, except for the expanded Pb–1.53Sb and the mould-cast Pb–1.8Sb alloy.

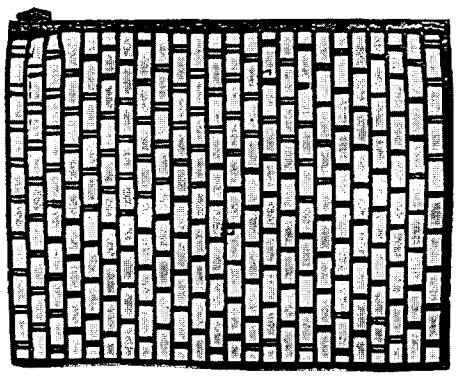

Fig. 11. Pb–1.8Sb concast battery grid after same cycle life test as in Fig. 10 with a new grid design that shows reduced vertical growth [8].

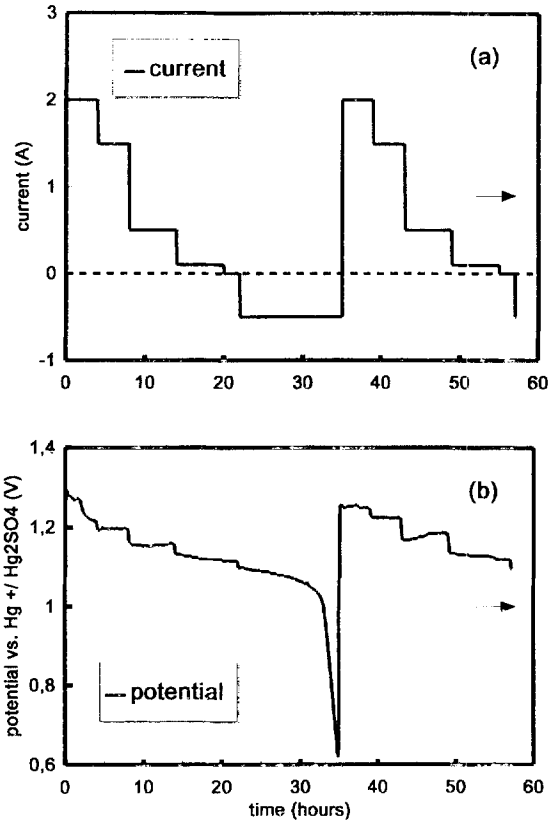

Fig. 12. Bare grids cycle corrosion test in 1.25 g/cm^3 H_2SO_4 at 60 °C: (a) current profile as a function of time, and (b) grid potential vs. time (45 days after start).

The weight loss of the different alloys is given in Fig. 13(a). The following results are obtained:

1. the concast and conventional antimonial grids show approximately 45% higher values than the antimony-free grids, except for the Pb–0.14Sr–0.25Sn grid, and
2. the weight loss for the Pb–1.53Sb grid was comparable with that of antimony-free concast alloys.

Table 1
Details of test alloys

	Sample	Thickness (mm)
1	Pb–1.8Sb (mould cast)	0.95
2	Pb–0.06Sr–0.24Sn–0.03Ag	0.85
3	Pb–1.8Sb	0.85
4	Pb–0.045Ca–0.4Sn	1.00
5	Pb–0.07Ca–0.60Sn–0.03Ag	1.00
6	Pb–0.07Ca–0.59Sn	1.00
7	Pb–0.07Ca–0.86Sn	1.00
8	Pb–1.53Sb (expanded)	0.90
9	Pb–0.06Sr–0.25Sn	0.85
10	Pb–0.14Sr–0.25Sn	0.85

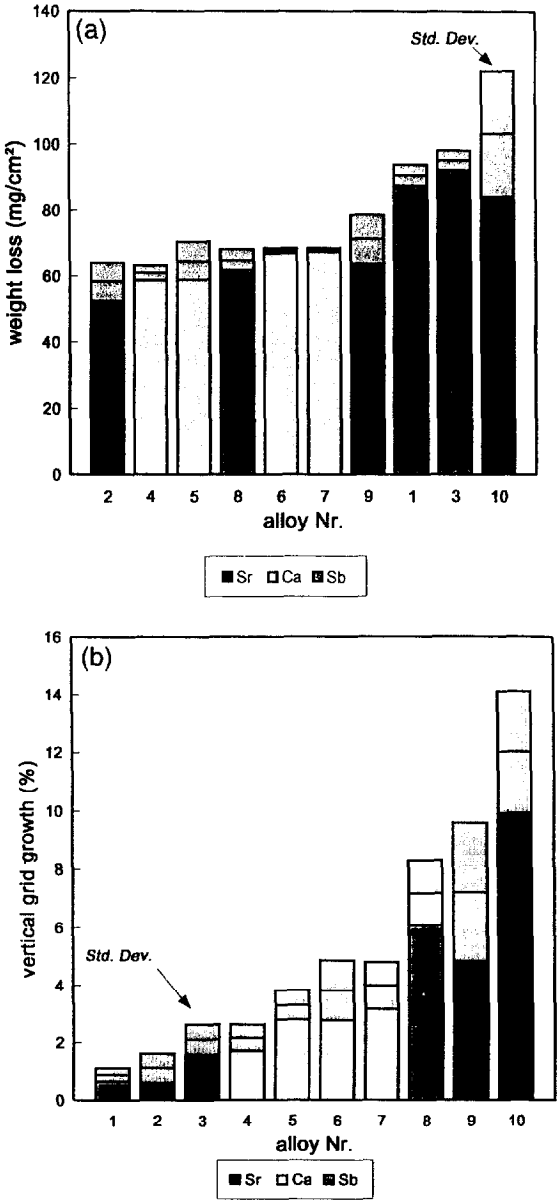

Fig. 13. (a) Weight losses and (b) grid growth of the alloys in Table 1 measured for the test procedure shown in Fig. 12.

Significant variations between the different alloys were observed in the vertical grid growth (Fig. 13(b)):

1. the lowest vertical growth value was measured for the mould cast Pb–1.8Sb and the highest values (above 7%) for the strontium alloys and the expanded antimonial alloy;
2. the expanded Pb–1.53Sb exhibited a high value for vertical grid growth, 7.2%, compared with 2.1% for the concast Pb–1.8Sb and 1.0% for the conventional Pb–1.8Sb;
3. the lowest grid growth value for the Pb–Ca–Sn alloys was observed for the alloy with the lowest calcium content, viz., Pb–0.045Ca–0.4Sn;
4. the addition of 0.03 wt.% Ag to the (low Sn) Pb–0.06Sr–0.25Sn composition produced a dramatic 85% reduction of the average vertical grid growth. The corresponding weight loss of 18% (Fig. 13(b)) was less impressive, and
5. for the concast Pb–0.07Ca–0.6Sn alloy, the addition of 0.03 wt.% Ag had little effect. There was a minimal reduction (4.6%) in the average weight loss and a reduction of only 13.1% in the average vertical grid growth.

Although some of the results listed above are already known for mould cast alloys, it is important to bear in mind that established knowledge from conventional casting systems concerning alloy composition properties and casting parameters may not be valid for continuous casting or alternative systems. A good example is the early negative experience with the OC corrosion and the poor mechanical properties of the Pb–1.8Sb concast (with or without nucleants).

In the case of strontium alloys that show the (fine/columnar grained) microstructure in Fig. 6, a strong intergranular corrosion attack was observed. As for the continuously cast Pb–0.18Ca–0.3Sn alloy reported in [15], the corroded thin Sr grids displayed a curvature with drum side concavity. This suggests that here the strength of the corrosion attack on the grid surface depends on the grain-boundary density [15]. A similar phenomenon was observed for the early low antimonial Pb–0.8Sb reported in Ref. [8]. Here, the higher corrosion rates on the fine-grained shoe side may have been enhanced by the presence of higher amounts of the non-uniformly distributed (antimony-rich) second phase. No grid warping was observed for the improved concast Pb–1.8Sb or the expanded Pb–1.53Sb alloys.

Minimal warping was exhibited by the Pb–0.06Sr–0.24Sn–0.03Ag grid cast with the same parameters as the warped Pb–0.06Sr–0.25Sn version. In this particular case, the silver addition appeared to have stabilized the microstructure and, thereby, increased the creep resistance. The beneficial effects of silver additions on lead–strontium alloys were reported in Ref. [16].

7. Battery tests

Grid growth was also evaluated from standard life tests, such as *DIN 43539* and *SAE J240* and cycle-life tests prescribed by car manufacturers.

Tear-down analysis of the cycled batteries showed that the highest vertical grid growth values were usually observed with the *SAE J240* test. Grid growth estimations for this test at 60 °C performed on a set of conventional and concast hybrid batteries (12 V 62 Ah, 450 A cca) showed:

1. 2.4% vertical grid growth for the concast versus 2.0% for the mould cast, and
2. 2.7% horizontal growth for the concast versus 1.4% for the mould cast.

The tendency to horizontal grid growth of the new grid design has a counterpart in a reduced grid growth in the

critical vertical direction, and thus reduces the danger of short-circuits on the upper grid frame.

The corresponding average cycle life to failure at 60 °C for the conventional batteries (4100 cycles) is somewhat higher than that of the concast (3700 cycles). A temperature-dependence curve for the number of *SAE J240* cycles as a function of temperature can be found in Ref. [17].

8. Field tests

To test the performance of concast hybrid batteries with low weight grids under practical conditions, a taxi fleet field test was started at the end of 1994. 108 series-produced batteries (12 V 100 Ah; 12 V 74 Ah) are being currently tested in eight German cities. The positive antimonial concast grid has a weight of 38 g (standard 54 g) and a thickness of 0.8 mm (standard 1.2 mm). The mileage-performance has ranged between a maximum of 9000 km/month and a minimum of 1920 km/month.

No battery failures were reported during the first 13 months; a result that fulfilled initial expectations. After 18 months, 13% of the batteries were recalled for inspection, 7% had failed and 80% were still in service.

9. Conclusions

Only a short time ago, continuous casting of lead–antimony alloys for positive grids (independently of the casting technology) was considered to be a rarity that belonged to the category of almost impossible tasks. Our experience shows that, basically, it is not impossible to obtain a corrosion stable microstructure for positive antimonial grids with the Wirtz concast system. The advantages are:

1. dimensional stability provided by a rigid frame;
2. creep resistance, deep cycling capability, rechargeability, and
3. grid design flexibility.

The disadvantages are the usual shortcomings ascribed to conventional antimonial grids. These are, depending on the antimony content, a higher rate of self-discharge and water loss.

In conclusion, the continuously-cast, lead–antimony grids developed by Hoppecke provide a real alternative to conventional mould casting in the continuous platemaking domain.

Acknowledgements

The authors would like to thank D. Hoffmann, H.J. Seibert and E. Schaum (production team) for their contribution to the project and J. Grothe and K.P. Wichartz for battery testing and evaluation. Useful suggestions from Dr J. Ruch and the technical assistance of H. Pack with the corrosion tests are also gratefully acknowledged.

References

[1] E. Cattaneo, R. Hennemann, W. Nitsche and J. Ruch, Electrochemical Engineering, *Proc. 3. Ulmer Elektrochemische Tage*, Ulm University Press, Ulm, 1996, p. 87.
[2] J. Wirtz, New developments in continuous cast grids, *Proc. 7th Int. Lead Conf., Madrid, Spain, 1980*; D. Lambert, *Batteries Int.*, (Oct.) (1992) p. 36; J. Wirtz, *Batteries Int.*, (Jan.) (1996), p. 56.
[3] E. Hoehne and H.D.v. Schweinitz, *Metallwirtsch., 21* (1942) 218.
[4] U. Heubner, I. Müller and A. Ueberschaer, *Z. Metallk., 66* (1975) 79.
[5] B.E. Kallup and D. Berndt, in K. Bullock and D. Pavlov (eds.), *Advances in Lead–Acid Batteries*, Proc. Vol. 84-14, The Electrochemical Society, Penington, NJ, USA, 1984, p. 214.
[6] N.Y. Tang and E.M.L. Valeriote, *J. Electrochem. Soc., 142* (1995) 2144.
[7] T.W. Caldwell and U.S. Sokolov, *J. Electrochem. Soc., 123* (1976) 972.
[8] E. Cattaneo, H. Stumpf, H.G. Tillmann and G. Sassmannshausen, *Batteries Int.*, (Oct.) (1996) 81.
[9] R.D. Prengaman, *Batteries Int.*, (Jan.) (1992) 52.
[10] H. Borchers, S.C. Nijhawan and W. Scharfenberger, *Metall, 28* (1974) 863.
[11] J.J. Lander, *J. Electrochem. Soc., 103* (1956) 1.
[12] J.L. Devitt and M. Myers, *J. Electrochem. Soc., 128* (1981) 1641.
[13] J.R. Mehta, *Proc. Symp Corrosion in Batteries and Fuel Cells*, The Electrochemical Society, Pennington, NJ, USA, 1983, p. 96.
[14] J.H. Hoover, *Batteries Int.*, (Jan.) (1996).
[15] D. Kelly, P. Niessen and E.M.L. Valeriote, *J. Electrochem. Soc., 132* (1985) 2533.
[16] N.E. Bagshaw, *J. Power Sources, 2* (1977/1978) 337.
[17] T. Yamada, Y. Nakazawa and N. Tsujino, *J. Power Sources, 38* (1992) 123.